PHOTONIC SENSORS / Vol. 4, No. 3, 2014: 215–219

Integrated Optical Waveguide Sensor for Lighting Impulse Electric Field Measurement

Jiahong ZHANG*, Fushen CHEN, Bao SUN, and Kaixin CHEN

Key Laboratory of Optical Fiber Sensing & Communications (Ministry of Education), University of Electronic Science and Technology of China, Chengdu, 611731, China

*Corresponding author: Jiahong ZHANG E-mail: zjh_mit@163.com

Abstract: A Lithium niobate ($LiNbO_3$) based integrated optical E-field sensor with an optical waveguide Mach-Zehnder interferometer (MZI) and a tapered antenna has been designed and fabricated for the measurement of the pulsed electric field. The minimum detectable E-field of the sensor was 10 kV/m. The sensor showed a good linear characteristic while the input E-fields varied from 10 kV/m to 370 kV/m. Furthermore, the maximum detectable E-field of the sensor, which could be calculated from the sensor input/output characteristic, was approximately equal to 1000 kV/m. All these results suggest that such sensor can be used for the measurement of the lighting impulse electric field.

Keywords: Lithium niobate, integrated optical waveguide, electric field sensor, Mach-Zehnder interferometer, bias control

Citation: Jiahong ZHANG, Fushen CHEN, Bao SUN, and Kaixin CHEN, "Integrated Optical Waveguide Sensor for Lighting Impulse Electric Field Measurement," *Photonic Sensors*, 2014, 4(3): 215–219.

1. Introduction

Integrated optical E-field sensors have been developed for electromagnetic compatibility (EMC) measurement since 1980s due to their negligible field distortion, high sensitivity, wide frequency response, and compact size [1–4]. However, the researches mainly focus on how to improve the sensitivity and bandwidth for the measurement of weak radio frequency (RF) E-fields. But, in some research areas, the E-fields are always pulsed E-fields which have fast rise time and intensive amplitudes. For example, in the area of high voltage engineering, the amplitude of the breakdown E-field for an air gap may be up to 1000 kV/m while the rise time is only a few microseconds; in the area of high power microwave, the E-fields have the amplitude range of 1 kV/m to 100 kV/m and typically have an ns-order rise time [5]. By contrast, the RF E-fields for the EMC measurement generally have amplitudes from 1 mV/m to several V/m, and their cutoff frequencies are usually from 10 kHz to several GHz. Therefore, the sensor used for the measurement of intense pulsed E-fields should not have a high sensitivity.

Some research works have been done to measure very high electrical fields. The electro-optic Kerr effect sensor has been used for the measurement of the pulsed intense E-fields in water [6]. The integrated optical-waveguide Pockels sensor has been used for the measurement of the intense electric fields [7]. However, these measurement systems must be constructed with many independent

Received: 31 March 2014 / Revised version: 5 May 2014

DOI: 10.1007/s13320-014-0189-9
Article type: Regular

optical components, which make the detection systems so sophisticated that limit their applications in practice.

We report in this paper a $LiNbO_3$ integrated optical waveguide Mach-Zender interferometer (MZI) based sensor. For the detection of the lighting impulse E-field, a tapered antenna has been designed, which is also used as the traveling wave modulation electrodes. Besides, we present here a novel bias phase angle control technique to control the sensor having a $\pi/2$ bias phase. Experimental results demonstrate that such sensor is suitable for the measurement of lighting impulse E-fields with amplitudes up to 1000 kV/m.

2. Design of the E-field measurement system

2.1 Measurement system

The configuration of the sensing system is illustrated in Fig. 1. The output of the tunable laser source is a linear polarized beam with a wavelength range from 1528 nm to 1563 nm. A polarization maintaining fiber (PMF) is used to connect the sensor to the output of the laser source. The sensor output modulated optical signal is transmitted to the optical coupler by a single mode finer (SMF). Then, 10 percent of the sensor output is converted into the electrical signal by the photo-detector one (PD1) and transmitted to the bias phase angle control unit for controlling the output wavelength of the tunable laser. Simultaneously, the 90 percent of the sensor output is sent to PD2 and an oscilloscope for extracting the detected electric field signal. Both the SMF and the PMF are long enough to ensure that the observation position is safely away from the intense electromagnetic pulse (EMP).

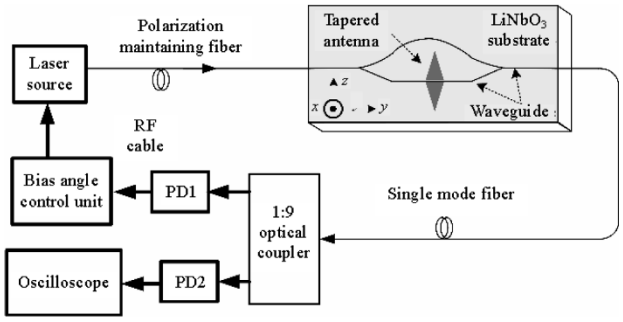

Fig. 1 Configuration of the integrated optical waveguide E-field measurement system.

2.2 Operation principles

The schematic of the sensor is shown in Fig. 2. Figure2(a) is the pattern of the tapered antenna, and Fig. 2(b) is the cross section view. When an E-field is received by the antenna, an induced voltage which depends on the intensity of the received pulsed E-field is applied to the modulating electrodes (the bottom of the tapered antenna). Then, the laser beam traveling through the MZI will be modulated by the induced voltage based on the Pockels effect of the $LiNbO_3$ crystal, as shown in Fig. 2(b). The output power P_{out} of the sensor can be written as [8]

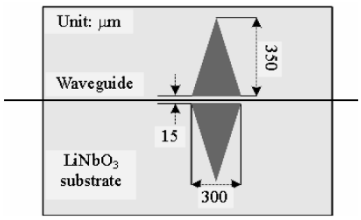

(a) Geometry of the tapered antenna

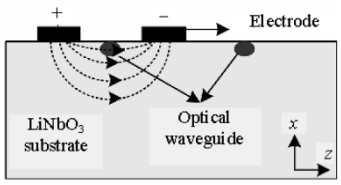

(b) Cross section view

Fig. 2 Schematic of the sensor: (a) geometry of the tapered antenna and (b) cross section view.

$$P_{out}=1/2P_{in}\alpha[1+\cos(\varphi(E)+\Delta\varphi_0)] \quad (1)$$

where P_{in} is the input optical power, α is the loss coefficient, $\Delta\varphi_0$ is the operating point (the phase mismatch under a zero E-field), and $\varphi(E)$ is the phase mismatch caused by the external E-field. If the operation point $\Delta\varphi_0=\pi/2$ and $\varphi(E)<<1$, then it can be described as

$$P_{out}=1/2P_{in}\alpha[1-\sin\varphi(E)]\approx 1/2P_{in}\alpha[1-\varphi(E)]. \quad (2)$$

As a result, the sensor output is linear with the input electric field.

Usually, the operation point $\Delta\varphi_0$ achieved by designing two arms of the MZI has a $\lambda/4$ length difference [1]. However, this imposes stringent fabrication tolerances which may be hard to meet. Besides, the bias phase angle will be changed along with the varying external conditions such as temperature, humidity, and so on [9]. Therefore, we propose here a novel operation point control method based on wavelength tuning. In order to make it possible to control the bias angle by wavelength tuning in the limited tunable wavelength range, an appropriate length difference ΔL has to be designed firstly. Then, the operation point can be rewritten as

$$\Delta\varphi_0=2\pi n\Delta L/\lambda+\varphi_0 \tag{3}$$

where n is the effective refractive index, λ is the operating wavelength, and φ_0 is the operation point drift value. According to (3), the optical bias angle $\Delta\varphi_0$ can be controlled as $\pi/2$ by changing the wavelength λ no matter what the bias drift φ_0 is. A schematic diagram of the bias angle control unit is shown in Fig. 3(a). And Fig. 3(b) is the assembled component side of the print circuit board (PCB) of the control unit. As shown in Fig. 3(a), the signal light source is a high performance continuous wave (CW) tunable laser covering 1528 nm to 1563 nm with high speed electronic tuning control (<10 ms, channel to channel), small trace tone frequency (<0.1 nm), and a simple RS232 interface which is used to communicate with the external control circuit. A low pass filer is used to extract the direct current (DC) component of the signal, and a log amp is used to provide the enough gain. The tunable laser is monitored by the micro-controller (C8051F410) which controls the wavelength seeping, acquires the maximum, minimum output optical power, and finally sets the wavelength which makes the sensor output become the mid value of the max and min as the optimum operating wavelength. More detailed operation principles of this bias angle control method have been analyzed in our precious paper [10].

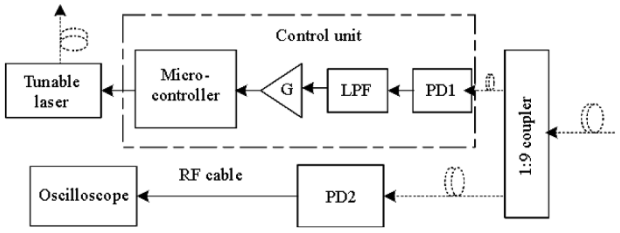

(a) Diagram of the control unit

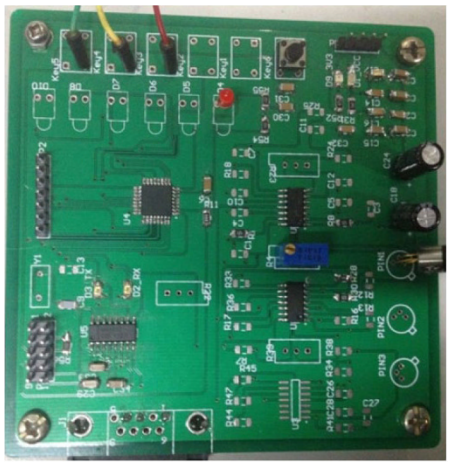

(b) PCB component of the control unit

Fig. 3 Diagram and PCB of the control unit: (a) diagram of the control unit and (b) PCB component.

3. Sensor fabrication and experimental results

3.1 Sensor fabrication

The sensor was fabricated on the *x*-cut *y*-propagating $LiNbO_3$ wafer crystal. The waveguides were fabricated by proton exchanging in benzoic acid with small amount of lithium and benzoate. Because the annealed proton-exchange process results in the extraordinary index being noticeably increased and the ordinary index being unnoticeably decreased, the waveguides fabricated on the *x*-cut *y*-propagating $LiNbO_3$ wafer crystal support only TE polarization. A SiO_2 film was coated on the waveguide by radio frequency magnetic sputtering as a buffer layer in order to reduce the transmission loss. The tapered antenna was formed on one of the two arms of the Mach-Zehnder interferometer by sputtering metals of Cr and Au and then electroplating Au. The photograph of one fabricated integrated optical

waveguide sensor is shown in Fig. 4. The package size of the sensor was (85 × 15 × 10) mm^3.

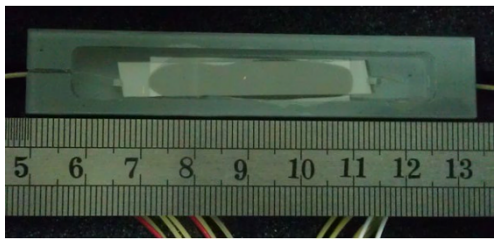

Fig. 4 Photograph of one fabricated E-field sensor after packaging and capsulation.

3.2 Experimental results

The sensor was calibrated under the standard lightening impulse with a front time of 1.2 μs and a tail time of 50 μs. The sensor shown in Fig. 1 was located between a simple pair of flat-plat electrodes which could be used to generate the uniform electric field. The flat-plat electrodes were connected with a high voltage pulse generator. Therefore, different electric fields could be obtained by changing the outputs of the high voltages generator and the distance between the two flat-plat electrodes. The experimental setup is shown in Fig. 5. As an example, Fig. 6 is one of the time domain responses of the measurement system, and it can be seen that the sensor output agrees well with the input E-field.

Fig. 5 Experimental setup.

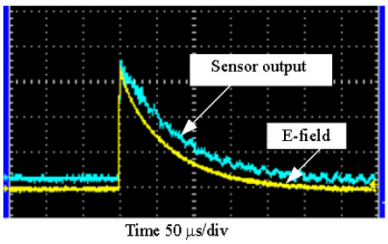

Fig. 6 Time domain response of the integrated optical sensor.

Furthermore, to study the input/output characteristics of the sensing system, different pulsed electric fields acquired by adjusting the outputs of the high voltage impulse generator and the distances between the two flat-plat electrodes were applied to the sensor. The output voltages of the sensing system were recorded by an oscilloscope with the 500-MHz bandwidth. The sensor outputs as a function of the input E-fields are shown in Fig. 7. A linear polynomial fitting has been done, and the correlation coefficient between the measurement and fitting was 0.9985 as the input electric fields varied from 10 kV/m to 370 kV/m. Considering the system noise level is about 10 mV and the signal to noise ratio is 3 dB, then the minimum detectable E-field of the measurement system was approximately equal to 10 kV/m. Besides, the maximum detectable E-field of the sensor that could be calculated according to the fitting curve was approximately equal to 1000 kV/m [11].

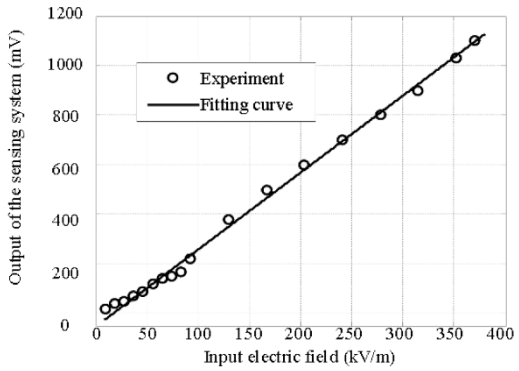

Fig. 7 Linear characteristics of the sensing system.

4. Conclusions

We present here a $LiNbO_3$ based integrated electro-optic sensor with an optical waveguide MZI and a tapered antenna. A novel bias phase angle control technique using wavelength tuning has been used to control the sensor which has a linear operation point. Experimental results show that such sensor has a potential for being used to detect the lighting impulse electric field with an amplitude up to 1000 kV/m.

References

[1] C. H. Bulmer, W. K. Burns, and R. P. Moeller, "Linear interferometric waveguide modulator for electromagnetic-field detection," *Optics Letters*, 1980, 5(5): 176–178.

[2] N. Kuwabara, K. Tajima, R. Kobayashi, and F. Amemiya, "Development and analysis of electric field sensor using $LiNbO_3$ optical modulator," *IEEE Transactions on Electromagnetic Compatibility*, 1992, 34(4): 391–396.

[3] T. Meier, C. Kostrzewa, K. Petermann, and B. Schuppert, "Integrated optical E-field probes with segmented modulator electrodes," *Journal of Lightwave Technology*, 1994, 12(8): 1497–1502.

[4] B. Sun, F. Chen, K. Chen, Z. Hu, and Y. Cao, "Integrated optical electric field sensor from 10 kHz to 18 GHz," *IEEE Photonics Technology Letters*, 2012, 24(13): 1106–1108.

[5] D. Nitsch, M. Camp, F. Sabath, J. L. Haseborg, and H. Garbe, "Susceptibility of some electronic equipment to HPEM threats," *IEEE Transactions on Electromagnetic Compatibility*, 2004, 46(3): 380–389.

[6] F. Banakhr, B. M. Novac, and I. R. Smith, "Electro-optic Kerr effect measurements of intense pulsed electric fields in water," in *Proceeding of IEEE Pulsed Power Conference*, Chicago, USA, June 19–23, pp. 328–333, 2011.

[7] T. Takahashi, "Electric field measurement just beneath a surface discharge by optical-waveguide pockels sensors," *Electronic Engineering in Japan*, 2003, 145(2): 28–34.

[8] R. C. Alferness, "Waveguide electro optic modulators," *IEEE Transactions on Microwave Theory Techniques*, 1982, 30: 1121–1137.

[9] J. P. Salvestrini, L. Guilbert, and M. Fontana, "Analysis and control of the DC drift in $LiNbO_3$-based Mach-Zehnder modulators," *Journal of Lightwave Technology*, 2011, 29(10): 1522–1534.

[10] J. Zhang, F. Chen, B. Sun, and C. Li, "A novel bias angle control system for $LiNbO_3$ photonic sensor using wavelength tuning," *IEEE Photonics Technology Letters*, 2013, 25(20): 1993–1995.

[11] B. Sun and F. Chen, "Experimental investigation of integrated optical intensive impulse electric field sensors," *Chinese Physics Letters*, 2009, 26(2): 024212.